Supplemental Online Material for

Rostral morphology of Spinosauridae (Theropoda, Megalosauroidea): premaxilla shape variation and a new phylogenetic inference

Mauro B.S. Lacerda[a,b,*], Orlando N. Grillo[c,*], and Pedro S.R. Romano[b,*]

[a]*Pós-Graduação em Zoologia, Departamento de Zoologia, Instituto de Ciências Biológicas, Universidade Federal de Minas Gerais, Belo Horizonte, Brazil.;*

[b]*Departamento de Biologia Animal, Universidade Federal de Viçosa, Viçosa, Brazil.;*

[c]*Museu Nacional, Universidade Federal do Rio de Janeiro, Rio de Janeiro, Brazil.*

*corresponding authors: Mauro B.S. Lacerda (mbslacerda@ufmg.br); Orlando N. Grillo (ongrillo@mn.ufrj.br); Pedro S.R. Romano (pedro.romano@ufv.br).

Geometric Morphometrics Methods

Acquisition of specimen's photographs

In our data set used for GMM and PM analysis, the photographs of *Angaturama limai* GP/2T-5, and *Suchomimus tenerensis* MN 6675-V (replica of the specimen MNN GDF501) were obtained in the Vertebrate Paleontology collection of the Departamento de Geologia e Paleontologia from Museu Nacional (MN/UFRJ), Rio de Janeiro, Brazil, by MBSL. The photographic protocol used to obtain the images of the specimens follows the three basic steps presented by Zelditch et al. (2012): (i) keeping the specimen surface in a horizontal plane with the camera lens; (ii) standardized scale; (iii) copies positioned at a fixed distance from the camera and in the center, aiming to settle or standardize any distortion. The photographs were taken with a Canon Rebel XS digital camera, fixed to a tripod, with an 18-55 mm lens (fixed at 55 mm) at a distance of 65 cm from the specimen whenever possible.

Photographs of specimen NHMUK PV R 16420, were provided by Angela C. Milner to our analysis. Other specimens' imagens were extracted from original and complementary literature: MSNM V4047 from Dal Sasso et al. (2005); MNHN SAM 124 from Taquet and Russel (1998) and additional images of SM of Hendrickx et al. (2016); *Baryonyx walkeri* NHMUK PV R 9951 from Charig and Milner (1997) and additional images of Hendrickx et al. (2016); *Cristatusaurus lapparenti* MNHN GDF 365 and MNHN GDF 366 from Kellner and Campos (1996), additional drawings of Taquet (1984) and additional images from SM provided by Hendrickx et al. (2016); and Spinosauridae indet. FSAC-KK-7281 from Lakin and Longrich (2019). The positioning of the specimens in the literature photographs was considered equivalent to our photography protocol, with perhaps only minor changes in the scale. Furthermore, the adjustment of the scale was done digitally in the program TpsDig2 (Rohlf 2015), allowing the removal of differences in the scale of the specimens (see text of the manuscript). Concerning the specimen FSAC-KK-7281, the description size and illustrated scale presented by Lakin and Longrich (2019) do not match, so, we consider the specimen size described by these authors.

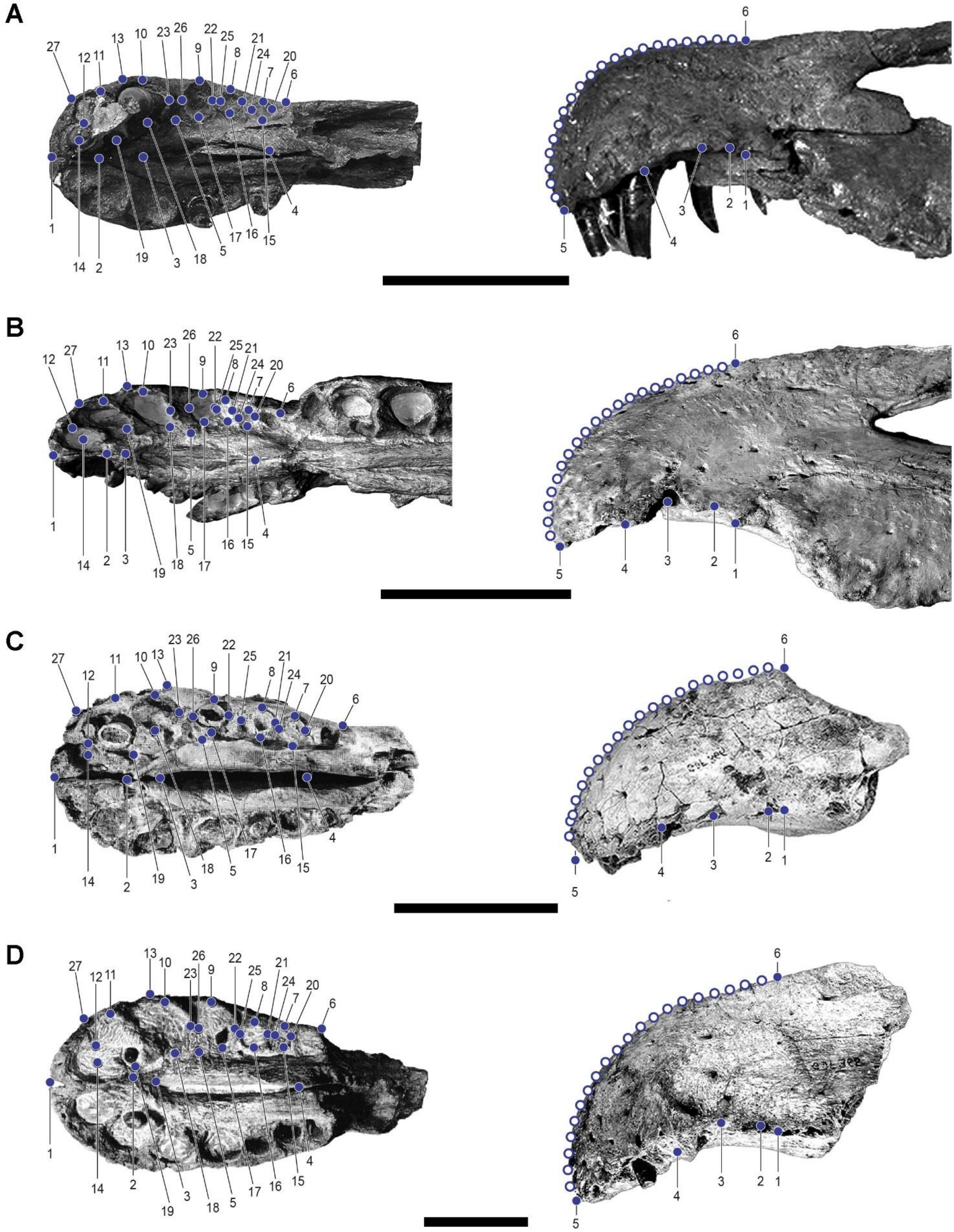

Figure S1. Premaxillae of *Baryonyx walkeri* NHMUK PV R 9951 (A), *Suchomimus tenerensis* MNN GDF501 (B, mirrored), and *Cristatusaurus lapparenti* MNHN GDF 366 (C) and MNHN GDF 365 (D) in ventral (left) and left lateral (right) views. Landmarks (filled blue circles; see Table 2 and Table 3 for LMs descriptions) and semi-landmarks (open circles). Scale bar = 100 mm. Images in (A) modified from Charig and Milner (1986). Images in (C) and (D) modified from Kellner and Campos (1996).

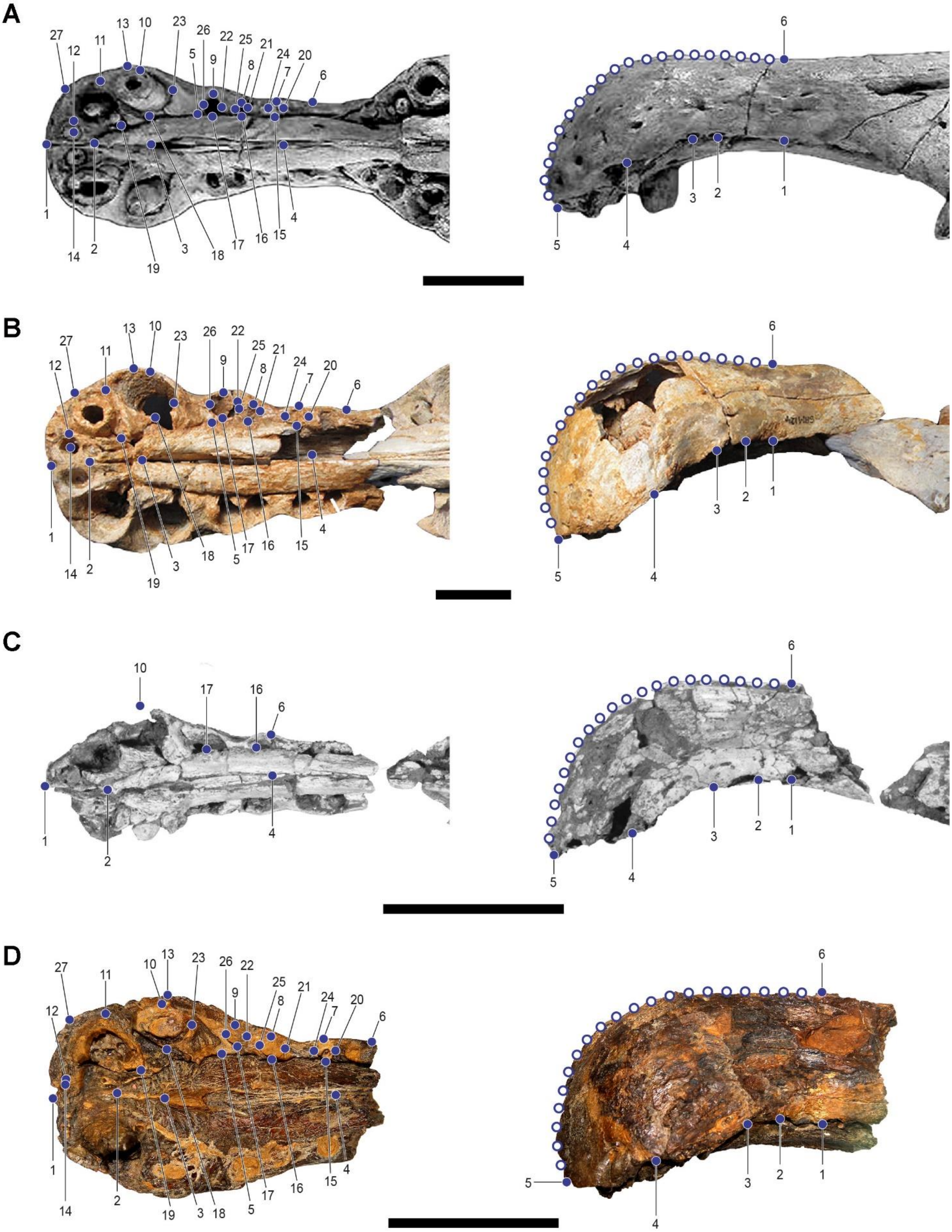

Figure S2. Premaxillae of the Spinosaurinae indet. MSNM V4047 (A), MNHN SAM 124 (B), NHMUK PV R 16420 (C), and *Oxalaia quilombensis* MN 6117-V (D) in ventral (left; A and C mirrored) and left lateral (right) views. Landmarks (filled blue circles; see Table 2 and Table 3 for LMs descriptions) and semi-landmarks (open circles). Scale bar = 100 mm. Images in (A) modified from Dal Sasso et al. (2005). Images in (B) modified from Hendrickx et al. (2016). Images credit Angela Milner (C) and Orlando Grillo (D).

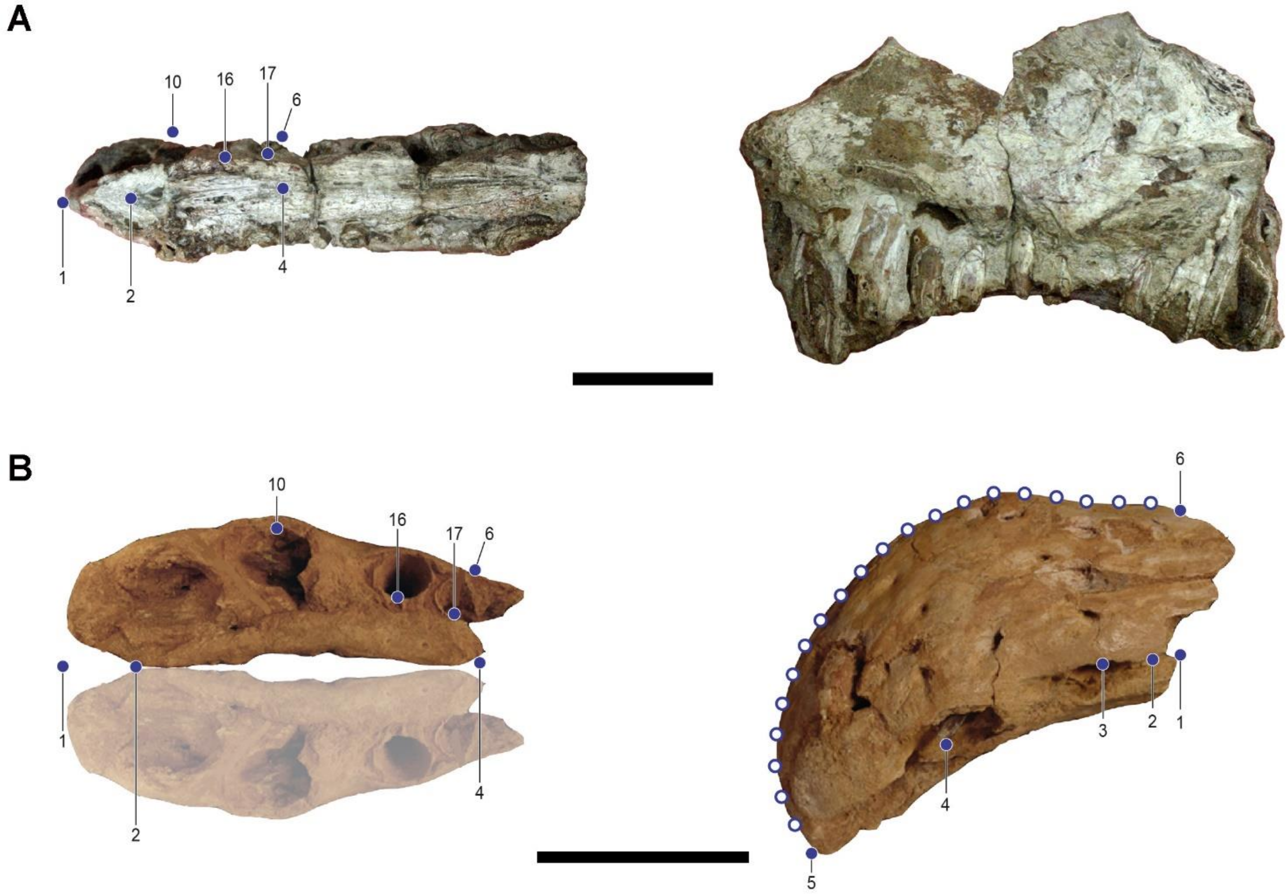

Figure S3. Premaxillae of *Angaturama limai* USP GP-2T/5 (A) and Spinosaurinae indet. FSAC-KK-7281 (B) in ventral (left) and left lateral (right) views. Lateral views mirrored from right side. Ventral view in B mirrored. Landmarks (filled blue circles; see Table 2 and Table 3 for LMs descriptions) and semi-landmarks (open circles). Scale bar = 50 mm. Images in (B) modified from Lakin and Longrich (2019).

Ordination analysis – additional supporting data

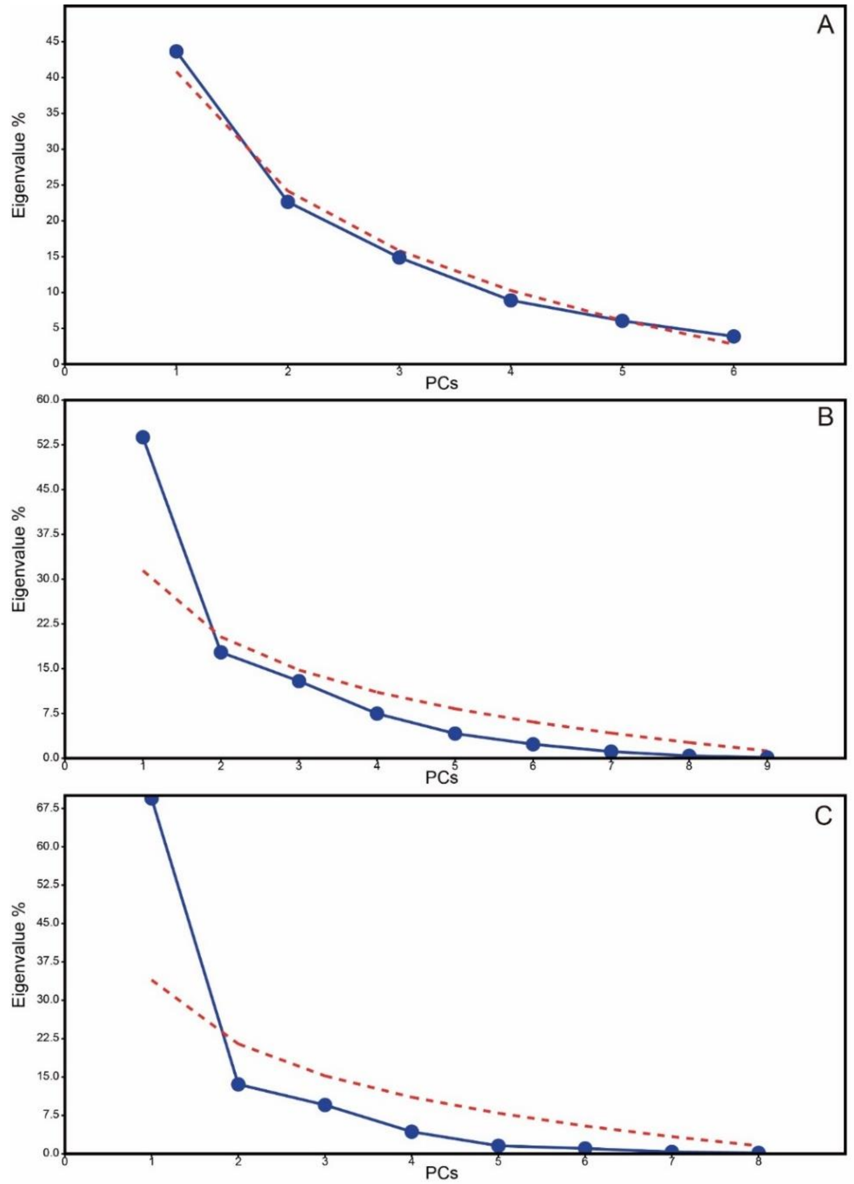

Figure S4. Percentage of variance of the principal components for the GMM analysis following the broken stick model (Jackson 1993). A) Ventral view, B) Additional ventral view, C) Lateral view.

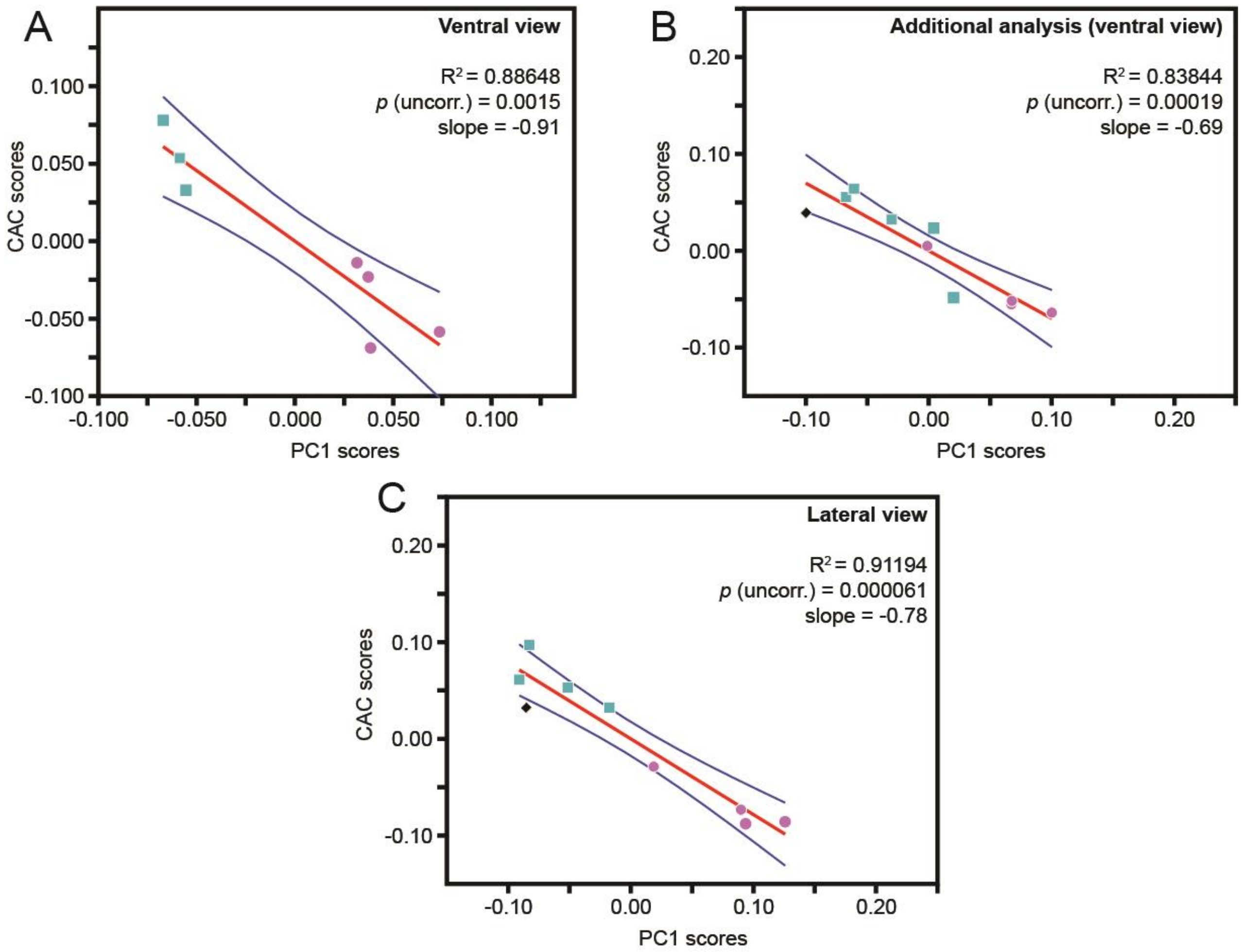

Figure S5. Regressions of PC1 scores and CAC scores of the three datasets analyzed. A) Ventral view, B) Additional ventral view, C) Lateral view. The regressions (red lines) fit into a bivariate linear model reconstructed based on Ordinary Least-Square algorithm and blue lines represent the 95% ellipse of confidence. Pearson's correlation coefficient (R2), p-value for null-hypothesis of uncorrelation between both variables (p), and slope (allometric coefficient) are given. Blue squares represent Spinosaurinae individuals and pink dots represent 'Baryonychinae' individuals. All regressions show clear correlation between the PC1 and CAC scores, close to isometry (specially the ventral view dataset). Thus, most of the variance in shape is interpreted as due to allometry. More details on the manuscript.

Phylogenetic Morphometrics

Cladistic analysis

We did not perform an extensive review of this character-taxon matrix because we consider it was already properly done (Carrano et al. 2012; Evers et al. 2015; Sales and Schultz 2017). However, by removing 50 OTUs, 304 characters became uninformative, which were deactivated using the WinClada v.1.61 (Nixon 1999-2002). Our searches were carried using the 50 remaining informative characters (they are: 6, 8, 10-13, 16, 23-24, 26, 45, 47, 83-84, 92, 100-101, 121-122, 139, 141-147, 149, 151-155, 159, 167-168, 180-182, 193, 196, 221, 239, 243, 272, 312, 314, 324, 353-354, see character list in Carrano et al. 2012 and Sales and Schultz 2017).

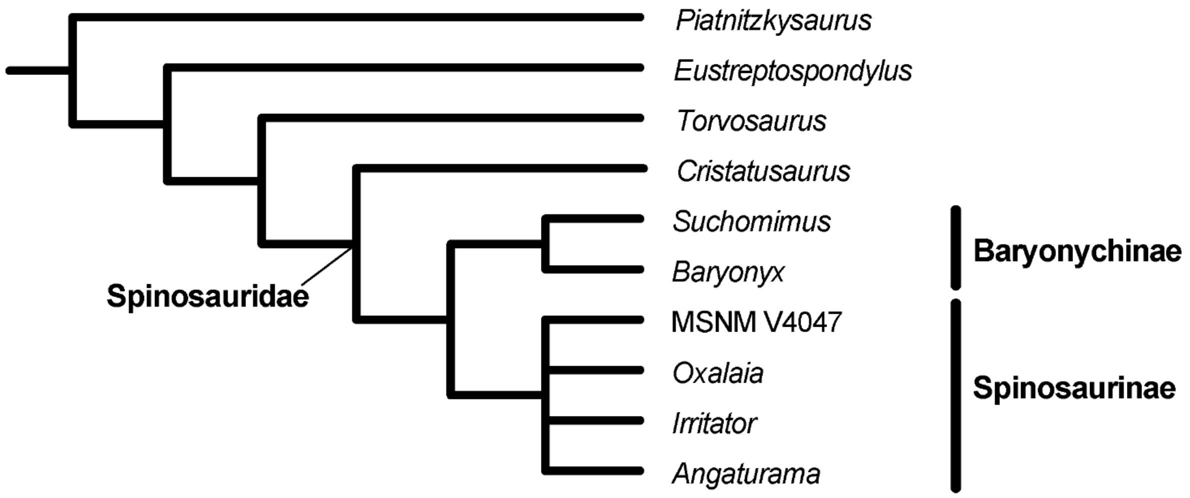

Figure S6. Strict consensus of 3 MPTs obtained with standard characters only.

Table S1. Comparison of different RFTRA realignment prior to heuristic searches performed in TNT using morphological characters (standard) and landmark-based characters (configurations) of the ventral view (VV) and lateral view (LV). All analyses were carried out following the same search strategies and both landmark-based characters were up weighted (=5)

RFTRA realignment	**Character inclusion**	***B. walkeri***	***C. lapparenti***	***O. quilombensis***	**MSNM V4047**	***Su. tenerensis***
Best score	VV + LV	86.695	86.829	**86.615**	86.697	86.710
	VV	**82.533**	82.556	82.612	82.537	82.568
	LV	79.161	79.274	**79.002**	79.160	79.142
MPT retained	VV + LV	1	1	1	1	1
	VV	2	1	1	1	1
	LV	1	2	4	1	1
MSNM V4047 + *Irritator* clade	VV + LV	Not found	Found	Found	Found	Found
	VV	Found	Found	Found	Found	Found
	LV	Not found	Found	Found	Found	Found
***Oxalaia* + *Irritator* clade**	VV + LV	Found	Not found	Not found	Not found	Not found
	VV	Found	Not found	Not found	Not found	Not found
	LV	Found	Found	Found	Not found	Not found

Premaxilla 'ancestral' shape

In the most recent ancestor of Baryonychinae (i.e. *Su. tenerensis* + *B. walkeri*), the 'ancestral shape' of the premaxilla, in ventral view, presents a large displacement of the interpremaxillary contact at the secondary palate, and in the middle-posterior portion of this structure. There is also a lateral expansion of the secondary palate as well as shape changes in the third (lingual border), fourth (labial border), and fifth (lingual and mesial borders) teeth of the premaxilla. The main changes in the lateral view are related to the position of the third, fourth, fifth, and sixth premaxillary teeth. In addition, there is a dorsoventral expansion/retraction of the dorsal-most and posterior-most portion of the premaxilla (referring to the end of the sLM curve and the LM6).

The 'ancestral shape' of Spinosaurinae premaxillae (i.e. *A. limai*, *O. quilombensis*, MSNM V4047, and *I. challengeri*) is not well defined as there is no data for *Angaturama limai* (the first branch to diverge). Therefore, the topology of this ancestor represents a mean between the ancestors of the clades Baryonychinae + Spinosaurinae and *O. quilombensis* + MSNM V4047 + *I. challengeri*. The 'ancestral shape' of Spinosaurinae premaxillae, in the ventral view, are concentrated in the region of the interpremaxillary contact at the secondary palate, and in the maximum width of the palate. These changes reflect in the sagittal position of the palate (assessed based on Lpm6). There are also changes in the shape of the second (labial border), fourth (labial and distal border), and fifth (labial and distal borders) premaxillary teeth. In the lateral view, the main changes are also in the sixth premaxillary teeth position. However, it is important to note the distinct morphology of the premaxilla of *A. limai* (presence of a sagittal crest), which was not considered in our analyses.

Finally, the major shape changes of the ancestor of the clade *O. quilombensis* + MSNM V4047 + *I. challengeri* are concentrated in the first tooth of the premaxilla, in the anterior region of the palate, and in the most extreme lateral expansion of the premaxilla. General shape changes also occur in the fourth and fifth teeth of the premaxilla. In the lateral view, the main shape changes occur in the anterior-most contour of the premaxilla in addition to shape changes in the third, fourth, fifth, and sixth teeth of the premaxilla, as already highlighted for the ventral view.

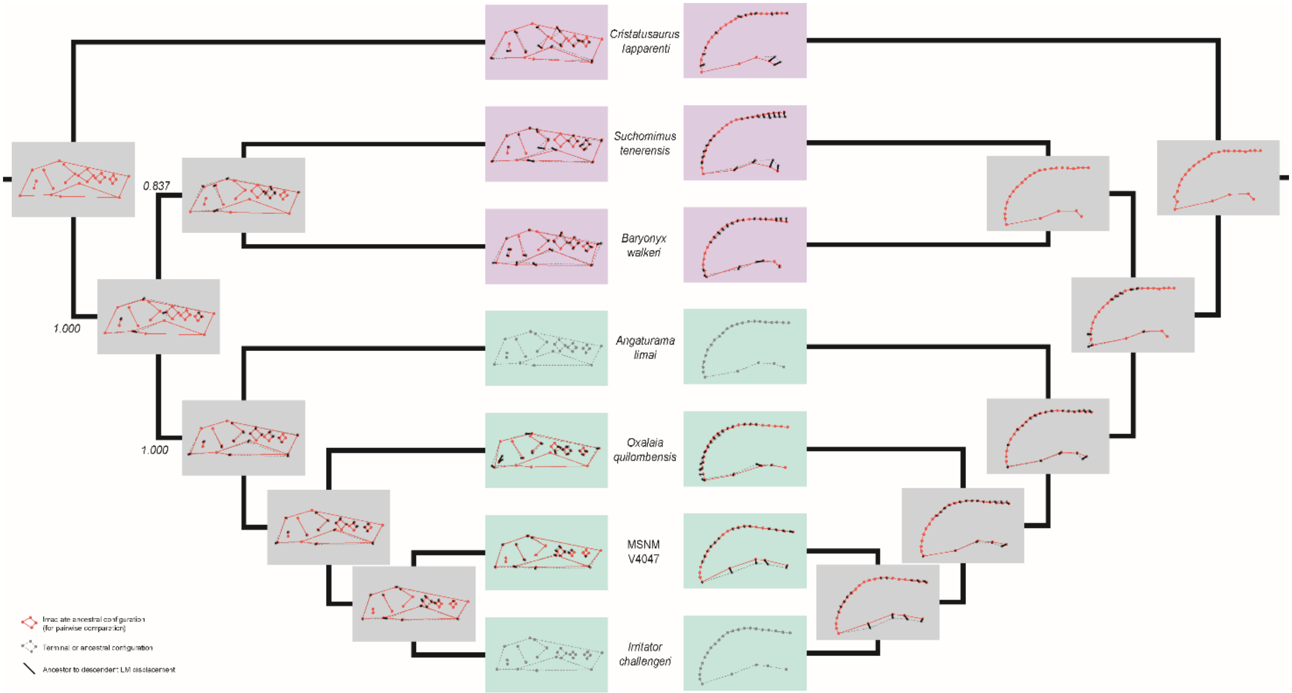

Figure S7. Most parsimonious tree (score=86.615) obtained by the analysis of morphological characters (standard) and landmark-based characters (configurations) of Spinosauridae species. In the left, ventral configuration; in the right, lateral configuration. The transformations of the ancestral shape of the premaxillary branches refer to the lateral view.

Data files

GMM data. Matrices with LMs coordinates; Procrustes coordinates, analysis and results of ordination methods and multivariate regression; **CAC data**. Matrices with LMs coordinates corrected by Common Allometric Component analysis; and **PM data**. Phylogenetic Morphometrics matrix combining standard characters and premaxillae configurations are available in Lacerda et al. (2021).

References

Carrano MT, Benson RBJ, Sampson SD. 2012. The phylogeny of Tetanurae (Dinosauria: Theropoda). Journal of Systematic Palaeontology, 10(2):211–300.

Charig AJ, Milner AC. 1997. *Baryonyx walkeri*, a fish-eating dinosaur from the Wealden of Surrey. Bulletin-Natural History Museum Geology Series, 53:11–70.

Dal Sasso C, Maganuco S, Buffetaut E, Mendez MA. 2005. New information on the skull of the enigmatic theropod *Spinosaurus*, with remarks on its size and affinities. Journal of Vertebrate Paleontology, 25(4): 888–896.

Evers SW, Rauhut OWM, Milner AC, McFeeters B, Allain R. 2015. A reappraisal of the morphology and systematic position of the theropod dinosaur *Sigilmassasaurus* from the "middle" Cretaceous of Morocco. PeerJ, 3:e1323.

Hendrickx C, Mateus O, Buffetaut E. 2016. Morphofunctional analysis of the quadrate of Spinosauridae (Dinosauria: Theropoda) and the presence of *Spinosaurus* and a second spinosaurine taxon in the Cenomanian of North Africa. PLoS One, 11(1):e0144695.

Jackson DA. 1993. Stopping rules in principal components analysis: A comparison of heuristical and statistical approaches. Ecology, 74(8):2204–2214.

Kellner AWA, Campos DA. 1996. First Early Cretaceous theropod dinosaur from Brazil with comments on Spinosauridae. Neues Jahrbuch für Geologie und Paläontologie-Abhandlungen, 199(2):151–166.

Lacerda MBS, Grillo ON, Romano PSR. 2021. Rostral morphology of Spinosauridae (Theropoda, Megalosauroidea): premaxilla shape variation and a new phylogenetic inference. figshare. Dataset. https://doi.org/10.6084/m9.figshare.14166467.v1.

Lakin RJ, Longrich NR. 2019. Juvenile spinosaurs (Theropoda: Spinosauridae) from the middle Cretaceous of Morocco and implications for spinosaur ecology. Cretaceous Research, 93:129–142.

Nixon, KC. 1999-2002. WinClada ver. 1.0000 Published by the author, Ithaca, NY, USA.

Rohlf FJ. 2015. The tps series of software. Hystrix, the Italian Journal of Mammalogy, 26(1):9–12.

Taquet P. 1984. Une curieuse spécialisation du cranê de certains Dinosaures carnivores du Crétacé: le museau long et étroit des Spinosauridés. Comptes-rendus des séances de l'Académie des sciences. Série 2, Mécanique-physique, chimie, sciences de l'univers, sciences de la terre 299(5):217–222.

Taquet P, Russel DA. 1998. New data on spinosaurids dinosaurs from the Ealy Cretaceous of the Sahara. Comptes Rendus de l'Académie des Sciences-Series IIA-Earth and Planetary Science, 327(5):347–353.

Zelditch MA, Swiderski DL, Sheets HD. 2012. Geometric morphometrics for biologists: A primer. 2ª Edition. USA: Elsevier. 478 p.